Benha Journal of Applied Sciences (BJAS) **print : ISSN 2356–9751**
Vol.(2) Issue(1) Oct.(2017), 65-82 **online : ISSN 2356–976x**

http:// bjas.bu.edu.eg

Petrology and Tectonic Setting of the Metagabbros and Granitoids Rocks of Muiswirab Area South Eastern Desert, Egypt

A.M.Mehanna, A.A.Rashwan, M.M.Mogahed and W.M.Saad
Geology Dept., Faculty of Science, Benha Univ., Benha, Egypt
E-Mail: arwaelgabry@gmail.com

Abstract

The Precambrian rocks of Muiswirab area in the southeastern desert –Egypt is consisting mainly of gabbroic rocks penetrated by syn-tectonic granitoids. Muiswirab metagabbros occurring as elongated huge mass subparallel with the regional tectonics of the area. These rocks show a partial alteration to one of these constituents' uralite gabbro, flaser gabbro/ amphibolite and retrograde of amphibolite. The best preserved parts of these metagabbros represent the dominant variety and show ophitic texture with pyroxenes and plagioclase as the major components. Subsequent alteration of these rocks ha s led to formation of uralitized pyroxene and amphibole and sometimes actinolite with plagioclase. Chemically, the present metagabbros always have tholeiitic affinities and show MORB/IAT i.e. transition tectonic setting. Moreover, they exhibit low Ti, Zr and Nb and REE contents this may indicate that, these rocks were generated in the back-arc marginal basin setting. The acidic calc-alkaline intrusive rocks from the studied area have geochemical characteristics of I-type granites with low Nb contents, a feature typical of arc-intrusive and pertaining to G_1 granitoids. The most important implication of the geochemical data from the present study is, that the investigated area pertaining to Juvenile Pan-African crust in the Nubian Shield.

Keywords: Muiswirab, Area, MORB, IAT, Calc, Alkaline, Backarc, Setting, Juvenile, Crust **.**

1. Introduction

The basement rocks of Egypt consist parts of the ANS and older crust. They cover an immense zone in the Eastern Desert, which stretches out southward to the Red Sea Hills of northern Sudan and a southern segment of the Sinai Peninsula, and smaller areas in the southern part of the Western Desert.

The main objective of the present paper is to investigate the rocks of G. Muiswirab area. This area is located in the South Eastern Desert of Egypt, and represents a small segment in Hamata Sheet (NG36D). Earlier geological studies on G. Muiswirab area have been limited to lithological mapping by [1]. The aim of the present work is to check and modify the EGSMA map and prepared a new map for the investigated area. Moreover, to shed more light on the petrology and chemical characteristics of the Muiswirab metagabbros and syn-orogenic granitoids. Finally, to decipher their origin (petrogenesis) and crustal evolution of the studied area.

Currently, the tectonic setting and crustal evolution are still the corner stone in understanding, classification and Knowledge of the rocks association and mineralization.

The investigated area (~90Km^2) is located in the upstream of Wadi El Gemal and represents the southern continuation of Hafafit culmination. It is bounded by Latitudes 24˚25`00˝ and 24˚28`53˝N, and Longitudes 34˚ 37` 0˝ and 34˚45`30˝E. This area is covered by late Precambrian rocks consist mainly of metagabbros and syn-tectonic granitoid rocks.

The post-granitic dykes and veins penetrated all the rock types and represented the last magmatic activities in the study area. The mapped area is traversed by three main Wadis, running roughly NNW-SSE, namely; Wadi El Drunkat, Muiswirab El Gemal and Huluz.

The area was studied in detailed and mapped on the scale 1:100,000 Fig (1) using aerial photographs scale 1:40,000, photomosaic scale 1: 50,000 and Landsat image scale 1:100,000.

2. General Geology of the area

The following rock units starting with the youngest are encountered:

- Dykes and veins
- Post tectonic granite G_2
- Gneissic tonalite
- Meta-andesite and their pyroclastics
- Metagabbros

2.1 The metagabbros

These rocks constitute the huge elongated mass of G. Muiswirab Fig (2) which follows a roughly E-W direction in the southern part of the map

Fig (1) They do not have intrusive contacts with the meta-andesites and their pyroclastics, whereas they are intruded by the gneissic granitoids. Based on the degree of deformation and metamorphic processes, two main varieties of these metagabbros are distinguished;

The first variety is the most abundant rocks of the exposure generally, they are massive and medium to coarse grained with hypidiomorphic texture, and their mineralogical composition which is plagioclase, pyroxenes and few hornblende. Rarely they are slightly foliated and metamorphosed Fig (3).

The second one is represented by moderately to highly sheared metagabbros, and consequently was subjected to more than one metamorphic episode, and transformed into one of these constituents, uralitized gabbro, flaser gabbro, amphibolite and retrograde of amphibolites Fig (4).

2.2 The gneissic tonalite

This rock is encountered at the north and west parts of the mapped area, they are intrusive into the metagabbros Fig (5) and meta-andesites and their pyroclastic rocks. These tonalitic rocks were dissected by several tributaries into isolated outcrops of varies dimensions. They are strongly foliated in the peripheral zone of the granitic outcrops but pass gradually into less deformed rocks inwards Fig (6). Rocks at the central part of the mass are granodioritic in composition, whereas those formed the outer and greater parts of the exposure are represented by tonalite. On the other hand, along the contacts between the present metagabbros and granitoid rocks, quartz diorite was recognized.

3. Petrography of the studied rocks

The following is a detailed petrographic description of these rocks with special emphasis on the metagabbros and gneissic granitoids.

3.1 The Metagabbros

These rocks represent the major rock unit of the area under consideration. Generally, the variation within these metagabbros arisen chiefly from the change in the relative amounts of the alteration products i.e. (the secondary minerals) and the intense of the deformation. Thus, they include four petrographic varieties, namely; metagabbros, uralitized gabbro, flaser and foliated amphibolite and retrograde of amphibolitized metagabbros

3.1.1 The less metamorphosed metagabbros

These rocks are the main rock variety of the present metagabbros. Microscopically, these rocks are medium to coarse grained with a hypidiomorphic granular texture Fig (7). They are composed mainly of calcic plagioclase ranging from bytwonite to labradorite (An_{65-80}), pyroxenes and little green hornblende. Sometimes, they show ophitic, subophitic and poikilitic textures Fig (8). Plagioclase occurs as colorless, subhedral longitudinal crystals, and occasionally with tabular forms. Pyroxenes are represented by hypersthene and augite. Hypersthene is usually predominating over augite, but in some samples this relation is reversed. Hornblende forms subhedral prismatic crystals and/or irregular patches of green color and is strongly pleochroic with pale green, green and dark green.

3.1.2 Uralitized gabbros

Uralitized gabbros are dominated in the western part of the outcrop. Microscopically, they are essentially, composed of varying proportions of saussuritized calcic plagioclase (average An_{70}); yellowish-brown secondary amphibole (uralite) with minor primary hornblende, and accessory actinolite, zoisite, magnetite and remnant pyroxenes, crystals retained as tiny cores in the uralitic amphiboles Fig (9). Plagioclase may still have subhedral or anhedral crystal forms showing faint carlsbad and albite twinning and incomplete extinction. Some crystals show twisted lamellae, and others are enclosed in the uralitized pyroxene, denoting an original ophitic texture relationship. Uralite, are frequently seen as interlocking brown hornblende anhedral crystals with weakly pleochroic from yellowish brown to brown. It forms a mantle around relics of pyroxene. The crystals sometimes enclose small prisms and laths of plagioclase. Some crystals are bordered by a thin actinolite sheath.

3.1.3 The flaser metagabbros and foliated amphibolite

A. The flaser metagabbros

These rocks are dominantly exposed along the NE-SW fault planes which parallel to elongated side of Gabal Muiswirab, thus they are characterized by flaser structure. On the other hand they are associated with the foliated amphibolite i.e. (intimately relationship). Generally, the flaser metagabbros are medium to coarse-grained with well-developed foliation and are greenish to reddish in color. Petrographically, they are mainly made up of plagioclase, hornblende, pyroxene and relics of chlorite and actinolite, with well-developed flaser texture Fig (10). Plagioclase, range in composition

from bytwonite to labradorite, it partly altered to saussurite. Hornblende is commonly greenish brown to green in color; it forms well oriented elongated crystals. Sometimes hornblende is replaced by chlorite. Pyroxenes form irregular remnant within pseudomorphic amphiboles and hardly to define the original mineral.

B. Foliated amphibolites

These rocks are associated with flaser gabbros with dark green-colored, rather medium to coarse grained rocks whose principle mineral components are hornblende and plagioclase, actinolite-tremolite, epidote and chlorite are additional subordinate components Fig (11) These types of rocks show well developed foliated texture. Hornblende is the most dominant, it occurs as bluish green to brownish green in color, subhedral prismatic crystals or aggregates separated by plagioclase crystals. Plagioclase ranges from labradorite to calcic andesine (Average An_{66}) in composition.

3.2 The Retrograde variety of amphibolitized gabbro

This rock dominantly exposed at the western flank of Wadi Huluz. Where, the minerals that constitute in foliated amphibolite are overprinted by low pressure/low temperature metamorphism. Thus, the minerals of this rock are represented mainly by actinolite, tremolite, chlorite, epidote and calcite.

The plagioclase is completely saussuritized Fig (12) Also some hornblende crystals merge into actinolite outward, while others are corroded by plagioclase crystals, and sieved by apatite and iron oxides.

3.3 The gneissic tonalite

The gneissic tonalites are medium to coarse-grained rocks. Moreover, these rocks show a gneissic texture where biotite and hornblende are oriented in parallel alignment **Fig (13)** They are composed essentially of oligoclase, quartz, biotite, and hornblende. Plagioclase forms slightly altered subhedral to anhedral crystals of oligoclase to andesine in composition. Some crystals are zoned. Quartz occurs as anhedral aggregates usually filling the interstices between other minerals, and show undulose extinction. Biotite is dark brown, rarely green in color with basal cleavage. It forms small flakes following the foliation planes in the rock and is partly altered to chlorite. Hornblende is green to dark green in color and often associated with biotite, chlorite and opaque minerals.

Granodiorites are grey to pale pink in color, medium grained hypidiomorphic texture. They are slightly to moderately deformed and weakly altered. Biotite is more abundant relative to hornblende and both increase toward the peripheries of the mass where the gneissic texture is more developed. These rocks are composed of quartz, plagioclase, sub amount potash feldspar, biotite and hornblende in decreasing order of abundance **Fig (14)** It is worthy to note that, along the contacts between the present metagabbros and gneissic tonalite, gneissic quartz diorite is encountered.

4. Geochemistry

4.1 Introduction

The geochemical characterization of the two main rock units encountered in the studied area is carried out through the study of the chemical composition of (31) selected samples representing, the Muiswirab metagabbros and gneissic granitoids. All samples (20) of metagabbros and (11) of gneissic granitoids were analyzed for their major and trace element contents **tables** (1, 2 and 3). Finally, eleven samples out of these were selected for their rare earth element contents.

Whole-rock chemical analyses of the powdered rock samples from the studied metagabbros and granitoids rocks were carried out in the Laboratories of Institute of the Mineralogy and Petrography, Hamburg University, Germany, for their major oxides, trace elements, and rare earth elements (REE).

Moreover, the CIPW norm values are computed from the analytical data according to method quoted by [2], and some statistical parameters are also calculated and presented in **table** (1and 3)

4.2 The chemical features of the present metagabbros

Based on the CIPW norm values of the various petrographic varieties of the examined metagabbros presented in **table (1),**

these rocks may be divided according to their chemistry into two groups, namely normative olivine metagabbros (group I) and normal metagabbros (group II).

4.2.1 Normative - olivine metagabbros (Group I)

They have a low differentiation index (D.I=Q+ Or+ Ab; after Thornton and Tuttle, 1960), ranging from 10.91 to 33.15 with an average 19.76. This may indicate that, the original magma of these rocks was primitive and tholeiitic in nature [3]. This interpretation is supported by the fact that Mg number [100Mg/Mg+Fe^{+2}] is between 57.69 and 71.35% with an average 64.51.

4.2.2 Normal Metagabbros (Group II)

They exhibit a slightly higher degree of fractionation (average Mg number ~ 62 and D.I. 13.24- 29.35 with average22.1), relative to group I.

4.3 Chemical classification of the studied metagabbros

The chemical classifications of the studied rocks follow two trends, the first uses the major oxides, while the second trend uses the normative minerals. Both trends are discussed in the following diagrams.

4.3.1 The (Na_2O+ K_2O) versus SiO_2 diagram

The present metagabbros include two varieties, namely normative-olivine metagabbros, and normal metagabbros. On the diagram **Fig (15)** suggested by [4] quoted in [5], shows that most of the analyzed samples are fall in the gabbro field, whereas, five samples of the two varieties are located just outside of the same field. These samples have too less contents of Na_2O and K_2O. Moreover, [6] used this relation to discriminate between alkaline and subalkaline composition. The data points of the studied metagabbros on the same diagram show clearly their subalkaline character.

4.3.2 Streckeisen's classification

Pl-(Opx+Cpx)-Ol and Pl-Opx-Cpx diagrams, suggested by [7], to differentiate between the different varieties of these metagabbros.

A. On the ternary diagram Pl-(Opx+ Cpx)-Ol Fig (16) The data points of the studied normative olivine metagabbros are plotted in the two fields, gabbro norite and olivine gabbro norite. The samples, which have less than 5% of normative olivine, hence they are corresponding to (the gabbro-norite) composition.

B. On the other hand, another diagram Fig(17) (Pl-Opx-Cpx) all the samples of normal metagabbros are located in the gabbro norite field. Moreover, the plots are spreading through the two subtype (leuco- and meso- gabbros), this depending on their enrichment of plagioclase contents.

4.3.3 Differentiation of the studied metagabbros

Several parameters accounting for the degree of magmatic differentiation were suggested by various authors. One of the most generally used parameter is the differentiation index (D.I) calculated after [8]. (D.I=Q+Or+Ab). The differentiation index is a measure of the basicity of an igneous rock; it is an ideal parameter for illustrating the variation in the chemistry of these rocks.

Some of the major oxides are plotted against the D.I. for illustrating the variation in the different oxides of the studied rocks. **(Fig)18** shows clearly that SiO_2, Na_2O and K_2O increase with increasing of the D.I., while MgO, CaO and Fe_2O_3 show a marked decrease with increasing D.I. On the other hand, Al_2O_3 and TiO_2 show scattering plots (no definite trend).

It is easy to recognized on the diagram (Fig)18 that a linear relationship is indicated between olivine metagabbros and normal metagabbros, suggesting a genetic link between the two rock varieties. Furthermore, the data points of the two varieties of the studied metagabbros are merged into each other's defining linear array (i.e. the absence of a marked chemical gap) with no differences in the distribution of the elements argues for a single comagmatic series.

4.4 Magma type of the studied metagabbros

On the AFM diagram which suggested by [9] to distinguish between tholeiitic and calc alkaline series Fig (19) Most of the present data points are located in tholeiitic field, except two samples only are plotted in calc-alkaline field, due to their slightly enrichment in their alkalies.

4.5 Tectonic setting of the studied metagabbros

Major and trace element contents, as well as certain elemental ratios are used to throw some light on the tectonic environments under which these rocks might have been formed. The following diagrams distinguish between two different rock series MORB type and island-arc type.

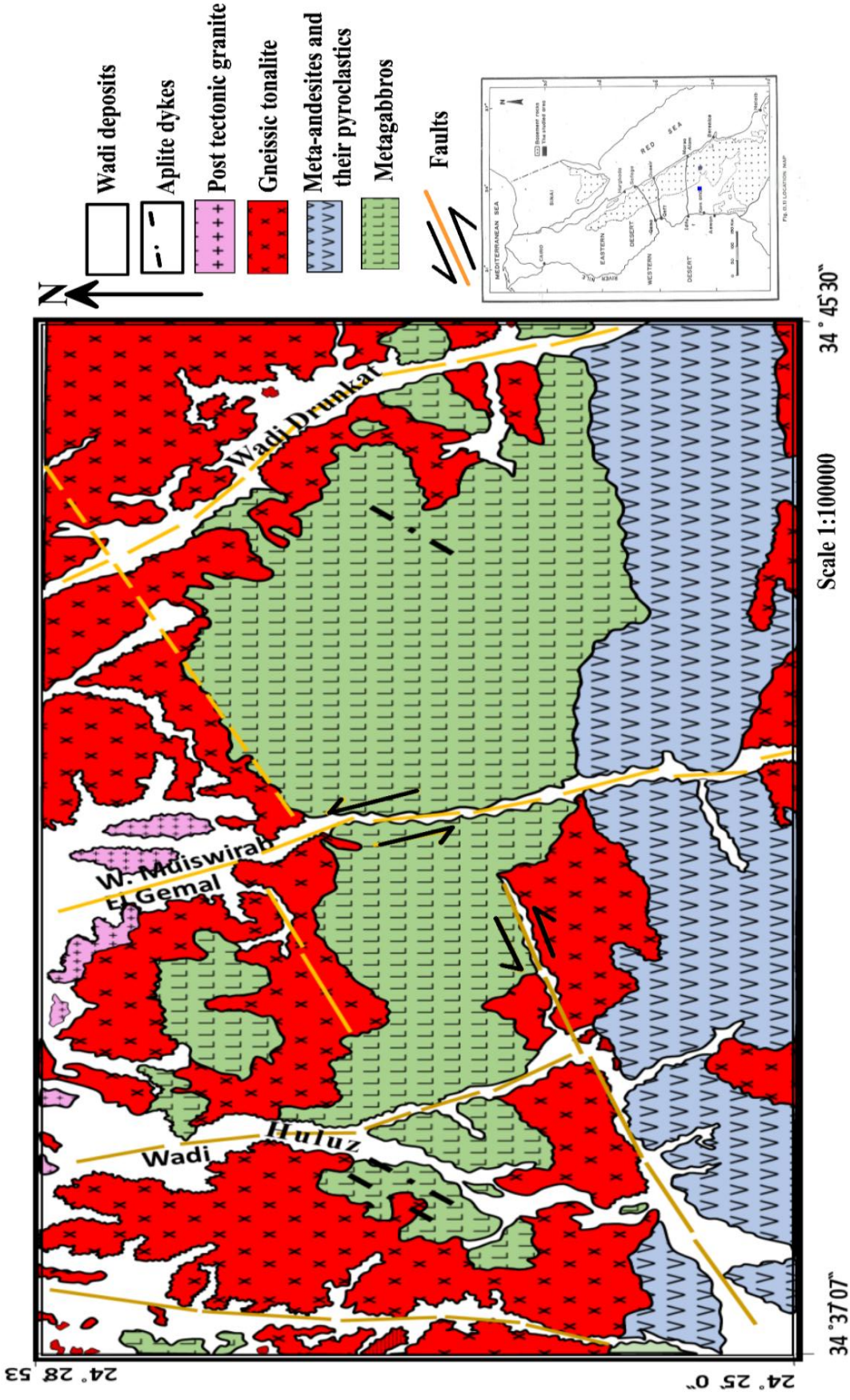

Fig(1) Geological map of the area under investigation.

Fig (2) Gabal Muiswirab as seen from Wadi Drunkat showing the summit in the background. (Looking to SW)

Fig (3) Photo showing the general view of massive and compact metagabbros (the first type). (Looking to S)

Fig(4) Photo showing well developed flaser structure in the metagabbros of Wadi Huluz. (Looking to NE)

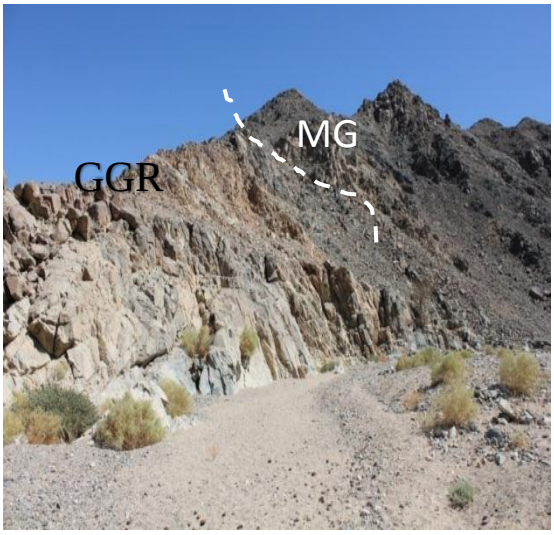

Fig (5) Photo showing the intrusive contact of the gneissic granitoids (white) (GGR) with the metagabbros (dark) (MG), along Wadi Huluz. (Looking W)

Fig(6) Photo showing well developed foliation in the gneissic granitoids, at the peripheral zone of its exposure. (Looking to E)

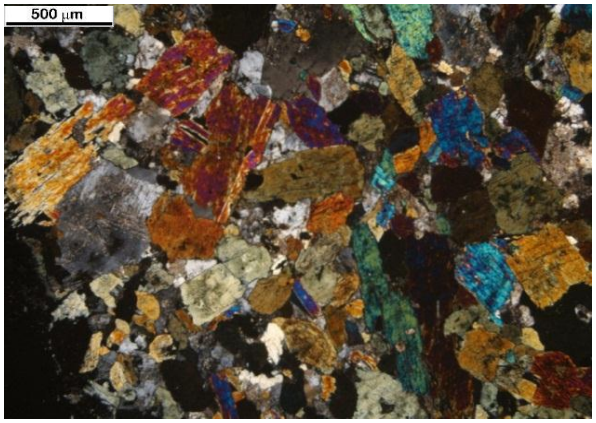

Fig (7) Photomicrograph showing hypidiomorphic granular texture and mineral composition of the present metagabbros (plagioclase, pyroxene (augite and hypersthene) and hornblende). (X.P.L).

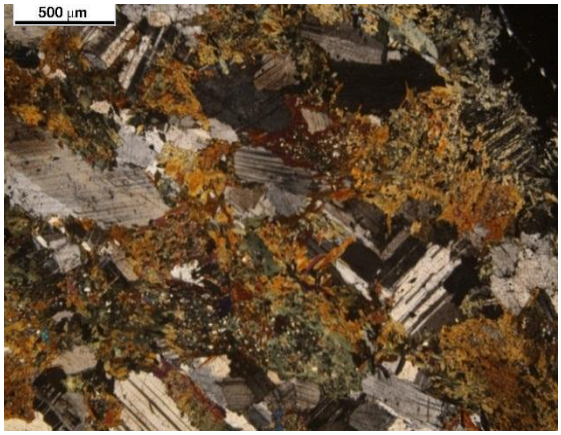

Fig (8) Photomicrograph showing ophitic and sub ophitic texture of the studied metagabbros. (X.P.L).

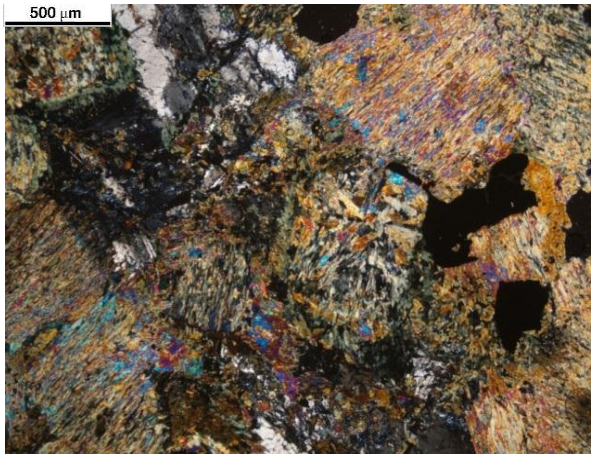

Fig (9) Photomicrograph showing the highly altered plagioclase, uralite and subordinate fibrous actinolite and opaques in the studied uralitized gabbros. (X.P.L).

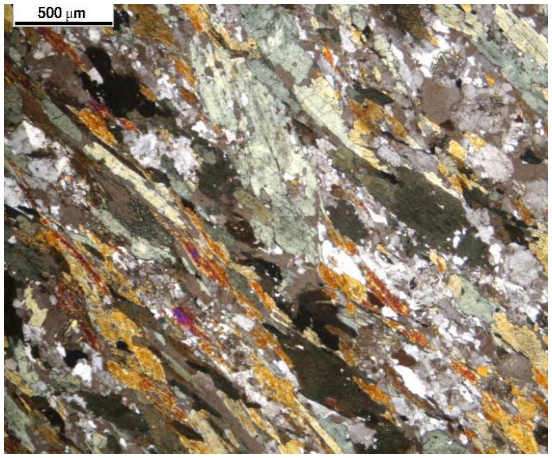

Fig (10) Photomicrograph showing well developed foliation in the coarse grained flaser metagabbros. (X.P.L).

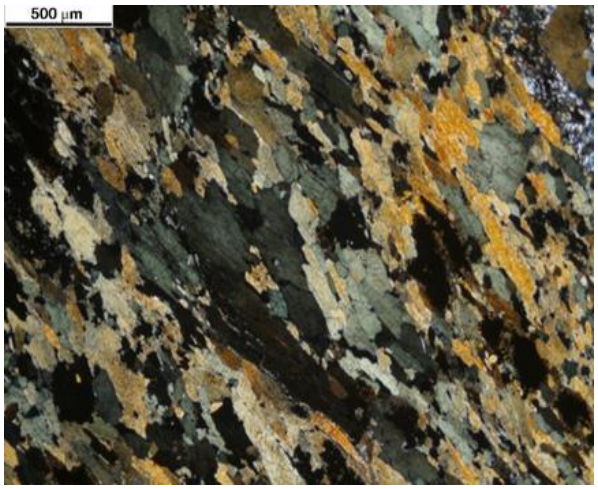

Fig (11) Photomicrograph in the present foliated amphibolite showing well developed foliation represented by amphibole minerals. (X.P.L).

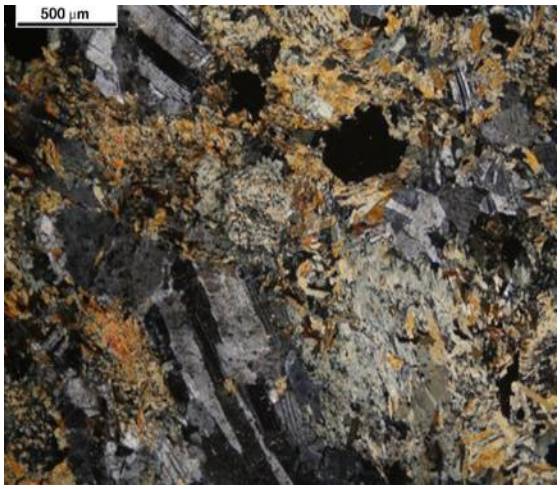

Fig (12) Photomicrograph showing the mineral composition of the present retrograde variety of amphibolitized gabbro (hornblende, plagioclase, tremolite and actinolite. (X.P.L).

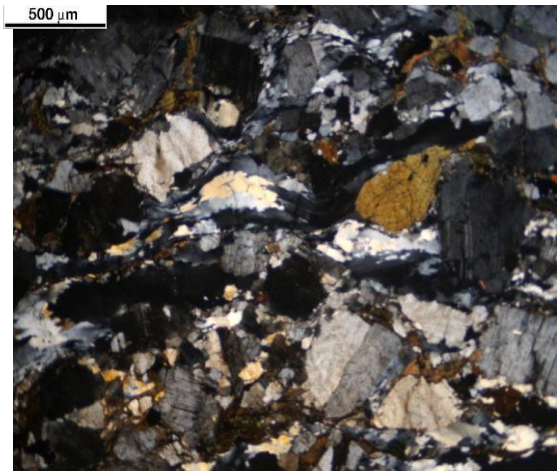

Fig (13) Photomicrograph showing mineral composition of the present gneissic tonalite (Plagioclase, quartz, biotite and hornblende). (X.P.L).

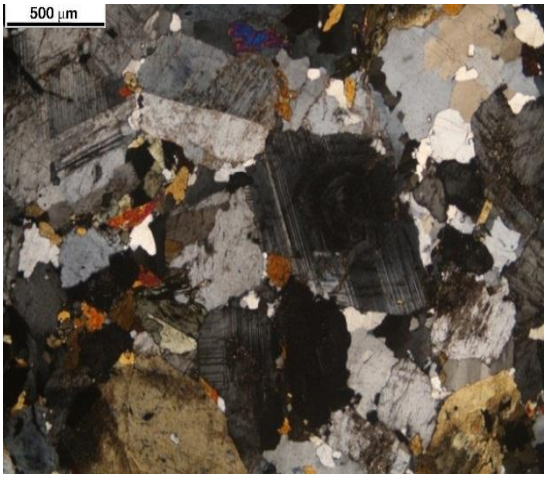

Fig (14) Photomicrograph showing mineral composition of the studied granodiorite (orthoclase, zoned plagioclase, quartz and hornblende). (X.P.L).

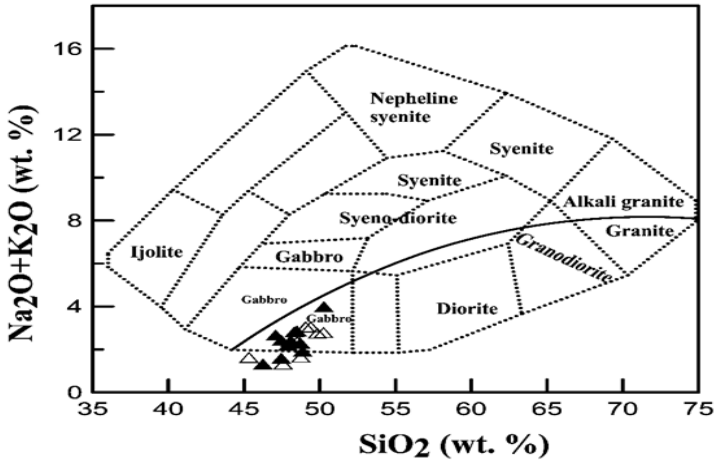

Fig (15) Classification of the studied metagabbros after [4]). The dividing line between alkali and sub-alkali magma series is after [6]. The symbol of normative olivine gabbro (▲) and the symbol of normal gabbro (△). The same symbols are used throughout the section dealing with the metagabbros

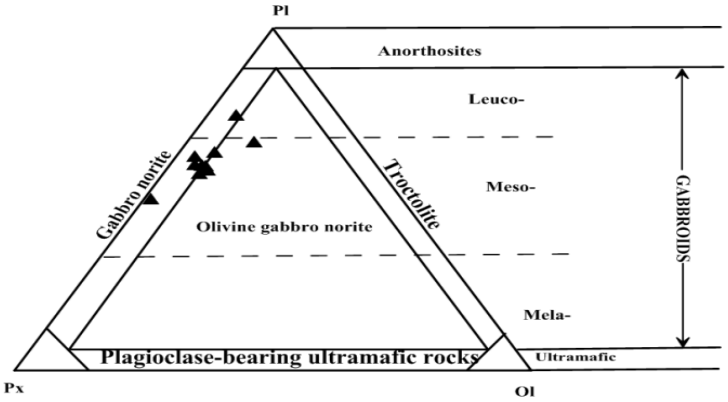

Fig (16) Classification and nomination diagram for the normative metagabbros [7].

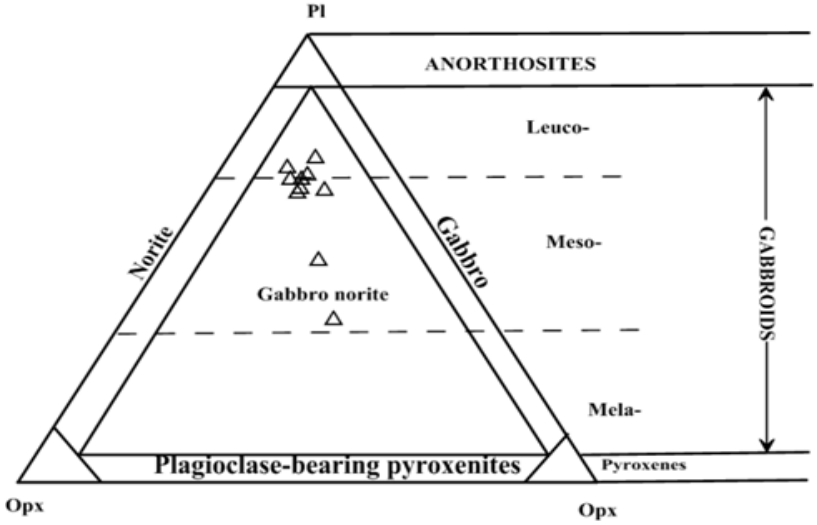

Fig (17) Classification and nomination diagram of the studied normal metagabbros [7].

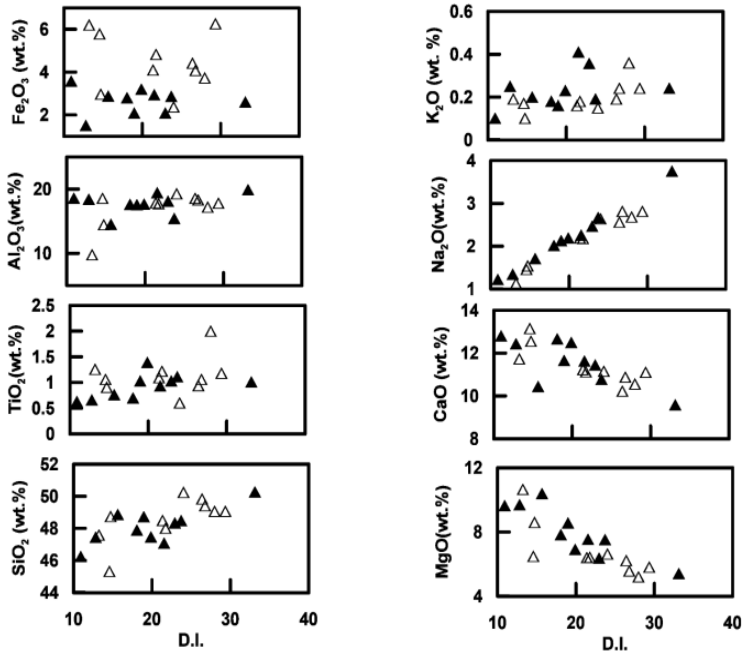

Fig (18) The relation between D.I. and the major oxides of the studied metagabbros after [8].

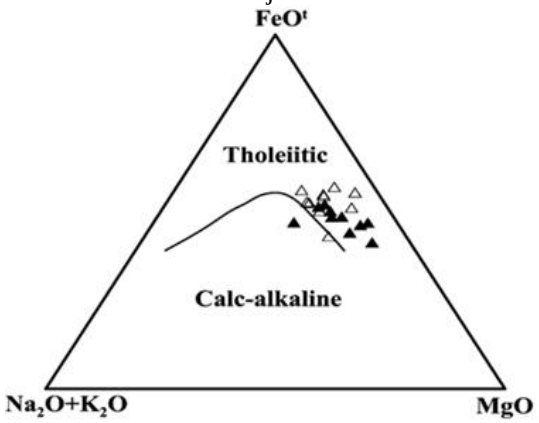

Fig (19) Plots of the samples of the studied metagabbros on the AFM ternary diagram after [9].

Table (1) Major element contents (wt.%) and normative components of the studied metagabbros

	Olivine metagabbros										Normal gabbros									
Sample No.	**w14**	**W9**	**W20**	**W58**	**3**	**27**	**W4**	**W5**	**W10**	**59W**	**1**	**7**	**13**	**17**	**18**	**19**	**21б**	**A 61**	**A 64**	**B 18**
SiO_2	47.90	46.24	47.45	48.73	48.87	48.48	47.47	47.08	48.33	50.27	48.75	49.84	50.24	48.50	48.02	49.41	49.06	47.58	49.07	45.32
TiO_2	0.70	0.63	0.66	1.03	0.76	1.11	1.39	0.93	1.03	1.01	0.91	0.94	0.60	1.09	1.22	1.06	1.18	1.26	2.00	1.06
Al_2O_3	17.57	18.56	18.40	17.54	14.51	15.42	17.64	19.41	18.11	19.89	14.43	18.56	19.29	17.84	17.72	18.32	17.80	9.75	17.21	18.54
Fe_2O_3	2.80	3.58	1.50	2.08	2.88	2.86	3.20	2.94	2.08	2.60	2.97	4.41	2.37	4.10	4.82	4.08	6.26	6.20	3.72	5.79
FeO	6.98	6.48	6.60	6.69	8.00	8.72	6.55	7.00	7.86	6.02	8.08	5.12	5.04	6.80	6.40	6.00	4.20	9.36	7.20	5.60
MnO	0.14	0.12	0.07	0.22	0.20	0.22	0.15	0.15	0.13	0.15	0.19	0.17	0.13	0.15	0.16	0.16	0.17	0.24	0.15	0.15
MgO	7.83	9.64	9.69	8.56	10.39	7.53	6.92	7.54	6.37	5.42	8.60	6.23	6.64	6.41	6.43	5.57	5.82	10.65	5.20	6.49
CaO	12.67	12.80	12.44	11.65	10.43	10.78	12.50	11.63	11.45	9.58	12.55	10.22	11.15	11.23	11.12	10.88	11.11	11.74	10.56	13.15
Na_2O	2.01	1.22	1.34	2.13	1.71	2.67	2.19	2.26	2.46	3.75	1.54	2.56	2.64	2.19	2.18	2.81	2.81	1.13	2.68	1.46
K_2O	0.18	0.10	0.25	0.16	0.20	0.19	0.23	0.41	0.36	0.24	0.10	0.19	0.15	0.16	0.18	0.24	0.24	0.19	0.36	0.17
P_2O_5	0.13	0.13	0.09	0.13	0.01	0.13	0.11	0.03	0.02	0.16	0.02	0.02	0.01	0.05	0.05	0.10	0.68	0.01	0.49	0.03
LOI	1.57	0.59	0.81	1.35	1.01	0.63	0.78	0.41	0.75	0.29	0.63	0.99	1.06	0.59	0.74	0.52	0.66	0.40	0.45	1.09
Total	100.48	100.09	99.30	100.27	98.97	98.74	99.13	99.79	98.94	99.38	98.77	99.25	99.32	99.11	99.04	99.15	99.99	98.51	99.09	98.85
$Na_2O+ K_2O$	2.19	1.32	1.59	2.29	1.91	2.86	2.42	2.67	2.82	3.99	1.64	2.75	2.79	2.35	2.36	3.05	3.05	1.32	3.04	1.63
FeOt	9.50	9.70	7.95	8.56	10.59	11.29	9.43	9.65	9.73	8.36	10.75	9.09	7.17	10.49	10.74	9.67	9.83	14.94	10.55	10.81
FeO^t/MgO	1.21	1.01	0.82	1.00	1.02	1.50	1.36	1.28	1.53	1.54	1.25	1.46	1.08	1.64	1.67	1.74	1.69	1.40	2.03	1.67
$FeO^t/MgO+FeO^t$	0.55	0.50	0.45	0.50	0.50	0.60	0.58	0.56	0.60	0.61	0.56	0.59	0.52	0.62	0.63	0.63	0.63	0.58	0.67	0.62
Mg#	64.72	70.23	71.35	68.07	68.17	58.91	62.92	63.69	57.69	59.40	63.67	64.50	67.99	59.67	60.50	58.94	64.91	63.84	53.56	62.63
																		Normative components		
Quartz (Q)	0	0	0	0	0	0	0	0	0	0	1.11	3.62	0.78	1.89	2.25	1.59	4.15	2.56	3.17	1.22
Orthoclase (Or)	1.06	0.59	1.48	0.95	1.18	1.12	1.36	2.42	2.11	1.42	0.59	1.12	0.89	0.95	1.06	1.42	1.42	1.12	2.13	1.00
Albite (Ab)	17.01	10.32	11.34	18.02	14.47	22.59	18.53	19.12	20.82	31.73	13.03	21.66	22.34	18.53	18.45	23.78	23.78	9.56	22.68	12.35
Anorthite (An)	38.39	44.87	43.45	37.83	31.33	29.53	37.62	41.61	37.32	36.73	32.17	38.59	40.34	38.37	38.03	36.67	35.25	20.97	33.87	43.53
plagioclase (Pl)	55.40	55.19	54.79	55.85	45.79	52.12	56.15	60.73	58.13	68.46	45.20	60.25	62.68	56.91	56.48	60.44	59.02	30.53	56.54	55.89
Diopside (Di)	19.12	14.25	14.24	15.42	16.42	18.85	19.08	12.86	15.85	7.92	24.29	9.57	12.00	13.75	13.51	13.44	12.09	29.93	12.44	17.13
Hypersthene (Hy)	11.84	16.30	16.96	16.94	27.72	13.24	11.15	5.57	10.95	10.10	20.87	15.47	17.32	16.89	15.58	13.58	9.76	22.56	14.03	12.04
Olivine (Fo)	3.77	4.71	5.08	3.03	0.81	3.62	2.09	7.60	3.45	3.18	0.00	0.00	0.00	0.00	0.00	0.00	0.00	0.00	0.00	0.00
Olivine (Fa)	2.04	1.76	2.30	1.45	0.39	2.60	0.98	4.09	2.70	1.95	0.00	0.00	0.00	0.00	0.00	0.00	0.00	0.00	0.00	0.00
Olivine (Ol)	5.81	6.47	7.39	4.49	1.20	6.23	3.07	11.70	6.15	5.14	0.00	0.00	0.00	0.00	0.00	0.00	0.00	0.00	0.00	0.00
Magnetite (Mt)	4.06	5.19	2.17	3.02	4.18	4.15	4.64	4.26	3.02	3.77	4.31	6.39	3.44	5.94	6.99	5.92	9.08	8.99	5.39	8.39
Ilmenite (Il)	1.33	1.20	1.25	1.96	1.44	2.11	2.64	1.77	1.96	1.92	1.73	1.79	1.14	2.07	2.32	2.01	2.24	2.39	3.80	2.01
Apatite (Ap)	0.30	0.30	0.21	0.30	0.02	0.30	0.25	0.07	0.04	0.37	0.05	0.05	0.02	0.12	0.12	0.23	1.58	0.02	1.14	0.07
D.I.	18.07	10.91	12.82	18.97	15.65	23.72	19.89	21.55	22.92	33.15	14.73	26.40	24.01	21.37	21.76	26.78	29.35	13.24	27.97	14.58

Mg# = 100* Molar Mg/(Mg+Fe); D.I.(Qz+Or+Ab refers to Differentiation index of Thronton and Tuttle (1960).

Table(2) Trace element contents (ppm) for the studied metagabbros

	Olivine metagabbros									Normal gabbros								
Sample No.	**w14**	**W9**	**W20**	**W58**	**3**	**27**	**W4**	**W5**	**W10**	**59W**	**1**	**7**	**13**	**17**	**18**	**19**	**216**	**A 61**	**A 64**	**B 18**
Nb	0.27	0.10	0.12	1.41	0.16	0.40	0.58	0.16	0.07	2.67	0.50	0.27	0.07	0.30	0.39	0.37	0.44	0.16	1.47	0.17
Zr	10.11	3.53	1.58	22.00	4.27	29 365	27.13	6.67	4.19	56.00	7.21	8.20	4.21	8.93	9.80	7.02	9.83	6.20	38.68	4.84
Y	2.78	2.56	1.25	18.22	6.15	19.07	8.58	3.41	5.06	19.11	7.92	7.32	3.88	7.80	7.37	7.74	14.77	9.24	19.11	6.42
Sr	479.76	322.12	355.45	422	236.42	172.14	442	432	371.20	438	237.22	431.32	368.92	348.37	339.22	408.59	405.89	411.84	425.89	313.99
Rb	1.89	0.83	0.61	2.54	2.25	1.12	6.42	2.65	2.76	1.75	1.21	1.44	1.15	0.96	1.73	1.83	1.77	1.94	2.30	0.66
Cr	98	117	157	364	320.11	222.42	116.70	114.56	189.83	412	320.26	184.51	217.71	154.46	155.26	112.82	147.07	163.80	157.47	113.72
Co	4	34	55	55	53.20	47.38	38.67	43.67	42.89	41	48.44	33.64	32.34	42.21	42.92	38.02	41.13	40.02	39.06	46.68
Ni	193	187	168	295	94.90	59.31	55.67	78.89	53.02	135	65.75	54.20	56.45	57.40	56.35	46.55	49.31	50.31	52.71	76.16
Cu	70.12	48.50	13.45	46	14.22	33.41	25.10	14.22	151.22	189	25.10	40.17	40.91	174.62	141.77	32.96	43.41	58.36	72.16	308.11
V	35	51	25	349	348.63	367.55	302	178	526.36	178	544.88	350.58	217.73	528.38	537.38	383.70	386.40	645.90	576.40	647.40
Zn	26.76	45.54	42.94	45	94	101.80	47.24	56.69	80.76	142	82.80	107.60	69.10	101.80	102.80	94.30	98.20	85.80	95.40	85.10
Hf	0.28	0.17	0.06	1.27	0.19	1.18	0.98	0.28	0.24	0.77	0.26	0.39	0.22	0.43	0.37	0.42	0.55	0.46	1.75	0.28
Pb	1.03	0.77	0.75	1.06	1.08	2.12	5.80	0.28	5.99	6.13	0.64	1.99	2.66	0.89	3.50	0.80	1.32	1.77	5.62	1.79
Th	0.06	0.06	0.05	0.07	0.03	0.16	0.44	0.11	0.08	0.64	0.06	0.05	0.01	0.03	0.04	0.06	0.07	0.18	0.44	0.03
Ta	0.05	0.05	0.06	0.06	0.02	0.44	0.08	0.09	0.02	0.15	0.21	0.02	0.01	0.02	0.02	0.16	0.03	0.02	0.15	0.12
Ba	54.94	11.96	16.22	123.00	22.37	41.97	245.04	33.08	44.32	153	19.93	37.23	23.41	27.51	44.49	30.98	33.92	41.88	73.48	39.15

4.5.1 FeO^t/MgO-Ni diagram

According to the conclusions of [10] the field of abyssal tholeiites which exhibit a higher rate of increasing Ni contents than those of island arc tholeiitic rocks. Plotting Ni versus FeO^t/MgO **Fig (20)** showed that the plots of the studied metagabbros fall within the area common of both island-arc and abyssal tholeiite fields, noting that, the samples which are pertaining to island arc fall just outside the boundary of abyssal field.

4.5.2 Ti-Cr diagram

Cr is considered as an immobile element and can successfully be used along with Ti to classify metavolcanic rocks into two tectonic domains, [11-12]. Also, [13] stated that, may not be greatly affected by alteration.

The diagram proposed by [11] distinguished between MORB and island arc lava. On plotting, the present data on this diagram **Fig(21)** the samples points representing the two varieties of the present metagabbros are located around the dividing line between two fields i.e. MORB and island arc lava fields.

From the foregoing, it is clear that the samples, which are located in the island-arc fields Figs (20,21), exhibit a slightly lower contents of Ni, Ti and Cr relative to the other examined samples.

4.6 Geochemistry of the granitoid rocks

Field and petrographic studies revealed that, the gneissic granitoids in the mapped area can be classified into two varieties namely gneissic tonalites, and gneissic quartz diorites. Noteworthy, the greater part of the gneissic granitoids exposure is built up of a gneissic tonalite rocks.

4.6.1 Normative components of the gneissic granitoids

The normative composition of the granitoid rocks as given in **table (3)** shows that, the gneissic tonalites are richer in differentiation index relative to its value of the gneissic quartz diorite, whereas the gneissic quartz diorite shows relatively higher contents of their normative (albite, anorthite and hyperthene) than those of the gneissic tonalite.

4.6.2 Chemical features of the granitoid rocks

The chemical data assist in characterizing the rock varieties and their magma source. The obtained data show clearly decrease in the abundance of SiO_2, K_2O, Rb, Zr and Hf from gneissic tonalites to gneissic quartz diorites, this is compatible with the increase of the magma differentiation from quartz diorite to tonalite. On the contrary, there is an increase of CaO, MgO, Fe_2O_3 $^{(t)}$, TiO_2, Sr, Zn and V contents from gneissic tonalites to gneissic quartz diorites. Accordingly, there is an increase in the plagioclase and ferromagnesian mineral contents to which, most of these elements are related, [14-15].On the other hand, Na_2O does not show a definite trend from gneissic tonalites to gneissic quartz diorites, this agrees with the fact that, in general, Na_2O does not vary systematically with differentiation progress [16].

4.6.3 Petrochemical classification of the present granitoid rocks

A. CaO- Na_2O- K_2O diagram

On this ternary diagram (**Fig)22** suggested by [17], the data points of two varieties (gneissic tonalite and gneissic quartz diorite) plot essentially in the tonalite field.

B. Ab- An- Or diagram

The plots of normative feldspar contents of the studied granitoids on the ternary diagram Fig (23) suggested by [18], the data points are located in the tonalite field with the exception two samples are located on the divided line between tonalite and trondhjemite fields.

4.6.4 Magma characteristics and variation diagrams

It has been generally inferred that the principal factor controlling the configuration of major oxides and trace element curves is related to fractional crystallization. Thus, using variation diagrams for the chemical components of the studied granitoids may help to clarify their geochemical characteristics and geotectonic environments.

A. Differentiation index versus major oxides

The major oxides SiO_2, TiO_2, Al_2O_3, Fe_2O_3, MgO, CaO, Na_2O and K_2O contents of the studied granitoids are plotted against the differentiation index after [8]. The relationships are shown on **(Fig)24** It is evident that the plots of the gneissic tonalite are clearly distinguishable from those of gneissic quartz diorite. They show a negative correlation of TiO_2, Al_2O_3, Fe_2O_3 and MgO with D.I. On the contrary, SiO_2 and K_2O are the only oxides which show a positive correlation with the D.I, whereas Na_2O does not appear to vary with the D.I. On the other hand the CaO contents are roughly constant or slightly decrease with the increase of the D.I. Generally, the investigated granitoids have normal trends, consistent with the general trend of differentiating granitic magma.

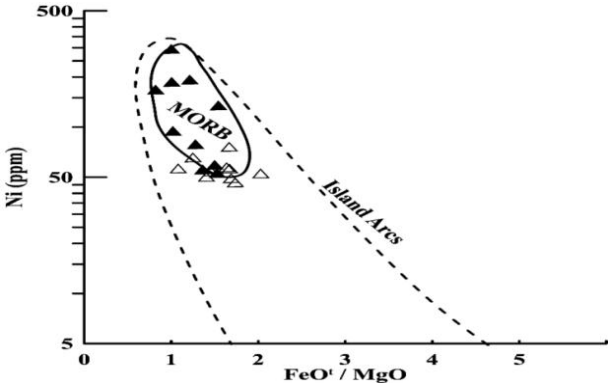

Fig (20) Plots of Ni (ppm) vs. FeO^t/MgO of the studied metagabbros on the diagram after [10].

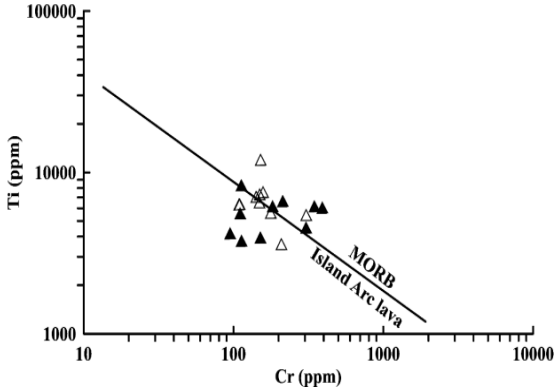

Fig(21) Plots of Ti (ppm) vs. Cr (ppm) of the studied metagabbros on the diagram after [11].

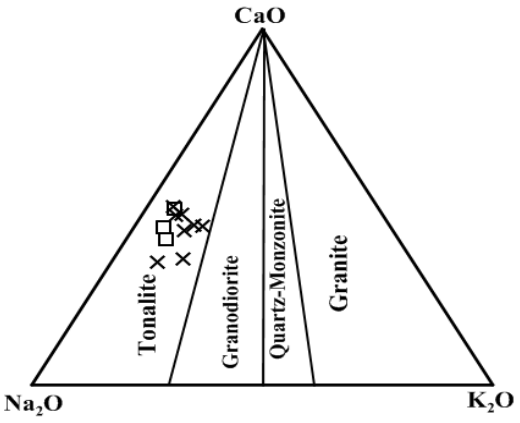

Fig (22) Na2O-CaO-K2O diagram for nomenclature of the studied granitoids [17]. (□ Gneissic quartz diorite and (✕) gneissic tonalite). The same symbols as shown here are used throughout the section dealing with the granitoids

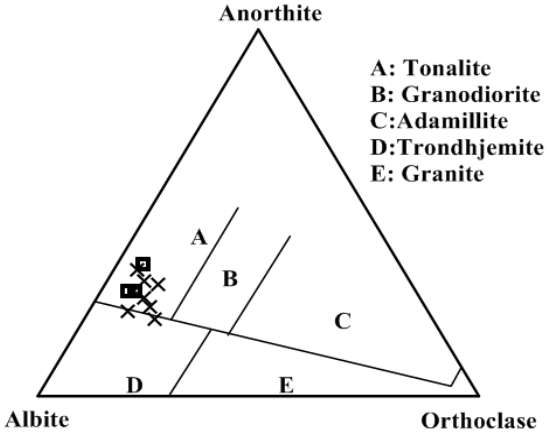

Fig (23) Ternary plot of normative contents for the studied granitoids, the classification boundaries, [18].

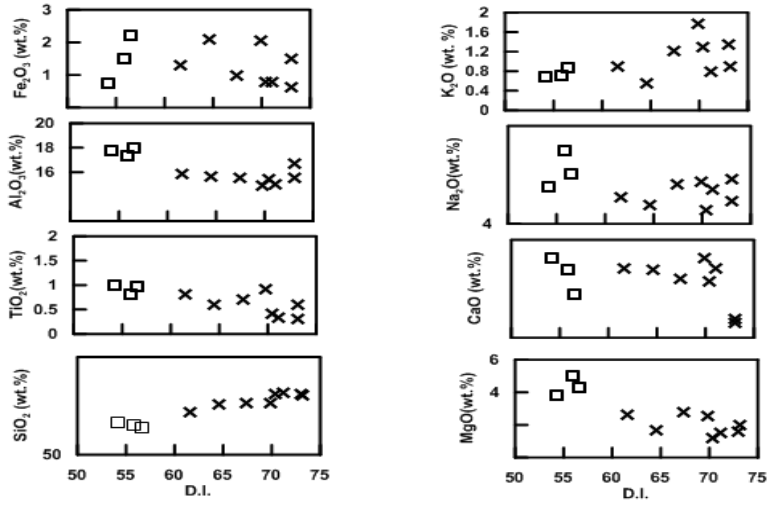

Fig (24) Variation of the major oxide contents (Wt. %) in the studied granitoids with D.I [8].

Table (3) Major (wt.%) and trace element (ppm) contents and normative components of the studied granitoid rocks.

Rock Type	Granodiorite				Tonalite				Qz-Diorite		
Sample No.	**A-57**	**15**	**w29**	**w56**	**30**	**1R**	**2R**	**3R**	**w32**	**w33**	**34w**
SiO_2	55.68	55.68	58.01	58.62	65.43	68.46	63.52	69.15	53.80	53.41	54.32
TiO_2	0.42	1.10	0.81	0.74	0.59	0.41	0.92	0.32	0.99	0.98	1.03
Al_2O_3	18.26	16.80	18.43	17.95	15.60	15.45	14.88	16.04	17.72	17.97	18.32
Fe_2O_3	2.42	2.69	0.71	0.93	2.09	0.79	4.86	0.78	0.74	2.20	3.12
FeO	3.50	4.40	5.28	4.60	3.00	2.40	0.81	1.50	6.60	5.53	5.02
MnO	0.12	0.07	0.11	0.11	0.12	0.07	0.09	0.06	0.12	0.13	0.12
MgO	5.26	5.62	3.64	3.74	1.68	1.20	2.58	1.50	5.83	5.27	4.98
CaO	9.40	7.48	6.85	6.38	4.93	4.52	4.85	5.00	8.84	9.07	7.83
Na_2O	2.80	3.78	3.93	4.17	4.37	5.28	4.35	4.69	3.26	3.43	3.79
K_2O	0.68	0.56	0.94	0.96	0.56	1.28	2.78	0.78	0.68	0.57	0.72
P_2O_5	0.06	0.09	0.18	0.21	0.11	0.12	0.28	0.10	0.12	0.16	0.12
LOI	1.01	0.63	0.87	0.87	0.84	0.85	0.81	0.97	0.89	1.14	0.78
Total	99.61	98.90	99.76	99.28	99.32	100.83	100.73	100.89	99.59	99.86	100.15
$Na_2O+ K_2O$	3.48	4.34	4.87	5.13	4.93	6.56	7.13	5.47	3.94	4.00	4.51
FeOt	5.68	6.82	5.92	5.44	4.88	3.11	5.18	2.20	7.27	7.51	7.83
FeO^t/MgO	1.08	1.21	1.63	1.45	2.91	2.59	2.01	1.47	1.25	1.43	1.57
$FeO^t/MgO+FeO^t$	0.52	0.55	0.62	0.59	0.74	0.72	0.67	0.59	0.55	0.59	0.61
Mg#	69.86	66.68	54.40	58.09	46.32	45.35	70.73	61.48	60.57	60.93	60.81
Normative components											
Quartz (Q)	9.5485406	7.5069089	8.9579941	9.6193223	24.257222	21.756941	16.152154	26.253712	2.7960532	3.8584888	4.8677347
Orthoclase (Or)	4.02	3.31	5.56	5.67	3.31	7.56	16.43	4.61	4.02	3.37	4.25
Albite (Ab)	23.69	31.99	33.25	35.29	36.98	44.68	36.81	39.69	27.59	29.02	32.07
Anorthite (An)	35.25	27.22	29.87	27.42	21.30	14.68	12.86	20.41	31.71	31.95	30.85
plagioclase (Pl)	58.94	59.20	63.12	62.71	58.27	59.35	49.67	60.10	59.29	60.98	62.92
Diopside (Di)	8.79	7.44	2.42	2.34	2.00	5.78	7.29	3.02	9.29	9.73	5.79
Hypersthene (Hy)	12.86	14.62	15.85	14.83	6.24	3.33	3.05	3.97	20.07	15.37	14.78
Olivine (Ol)	0.00	0.00	0.00	0.00	0.00	0.00	0.00	0.00	0.00	0.00	0.00
Magnetite (Mt)	3.51	3.90	1.03	1.35	3.03	1.15	0.24	1.13	1.07	3.19	4.52
Ilmenite (Il)	0.80	2.09	1.54	1.41	1.12	0.78	1.75	0.61	1.88	1.86	1.96
Apatite (Ap)	0.14	0.21	0.42	0.49	0.25	0.28	0.65	0.23	0.28	0.37	0.29
D.I.	37.26	42.80	47.77	50.58	64.54	74.00	69.39	70.55	34.40	36.25	41.19
Nb	1.01	0.78	3.34	1.07	1.07	3.5	6.4	2.3	2.43	2.64	3.18
Zr	52.02	26.03	105	139.47	139.47	120	291	120	89.56	85.99	74.87
Y	9.66	8.10	9.73	32.67	32.67	19	8	9	14.83	17.28	12.84
Sr	353.39	834.72	631	205.39	205.39	455	341	502	527	631	677
Rb	10.87	4.99	15.34	5.51	5.51	23	60	16	10.11	7.12	9.3
V	159.75	268.43	116	109.55	109.55	42	33	5	207	210	168
Th	0.41	0.70	1.17	1.28	0.27				0.93	1.06	0.81
Ba	175.83	107.63	351	324.00	121.33	275	450	215	235	215	245

Mg# = 100* Molar Mg/(Mg+Fe); D.I.(Qz+Or+Ab refers to Differentiation index of Thronton and Tuttle (1960).

B. AFM diagram

On the AFM diagram Fig (25) after [9], it is clear that the investigated granitoids follow a typical calc-alkaline trend, being relatively rich in total alkalis. Moreover, there is a continuous trend of differentiation from quartz diorite to tonalite.

Furthermore [19] used the same diagram to differentiate between compressional and extensional environments i.e. granites formed under environments of compression (e.g. subduction related granites) and those formed under tensional condition (e.g. interaplate rift environments). Also, they mentioned that, the trends of compressional suites tend to be more or less perpendicular to the FM- side line for the entire trend. It is observed that the trend of the present granitoids is nearly perpendicular to the FM-side line indicating that the present granitoids were generated under compressional environment.

Additional evidence for the calc- alkaline nature of these granitoids comes from the fact that the agpatic index (AGP=Na+K/ Al) for all the granitoid samples (quartz diorite and tonalite) is less than 1, it ranges from 0.48 to 0.67.

c – S- and I- type granites

Fig(26) shows the fields of S- type and I-type granites using the relationship between Na_2O % and K_2O% [20]. On this diagram all the data points of the studied granitoids fall in the field I-type granites (i.e. granites essentially of magmatic origin).

4.6.5 Trace elements variation diagrams

Since trace elements such as Nb, Zr and Y are reliable indicators for the nature of the original magma of a given suite of rocks as they are relatively immobile, they are here used in an attempt to clarify the origin and the evolution of the present granitoids.

a- SiO_2- Rb/Zr diagram

[21] used the relation between SiO_2 and Rb/Zr ratios to discriminate between the I-type and S-type granitoids **Fig (27**) The plots studied samples fall clearly within the I-type volcanic arc granitoids (VAG).

b- Nb-SiO_2 diagram

On the Nb-SiO_2 diagram **Fig (28)** suggested by [11], the gneissic quartz diorites and gneissic tonalites samples fall in the field of volcanic- arc magma.

Regarding to [11] who stated that "the igneous rocks of all SiO_2 values that formed above active Benioff zones have Nb contents below 15 ppm, whereas for granitic products of within-plate continental magmatism with SiO_2 contents between 60 and 75 %, Nb lies in the range of 50 to 500 ppm. The studied granitic rocks have average Nb contents below 15 ppm. It is argued by [22] that " in a subduction zone setting [23], the mantle above the descending oceanic lithosphere slab would be modified by low-Nb fluids, and would not, on melting produce acidic melts enriched in Nb. In contrast, any magmatism of a within-plate variety could progressively enrich melts in Nb". Considering the criteria suggested above it may be concluded that all the present granitoids were generated above subduction zones.

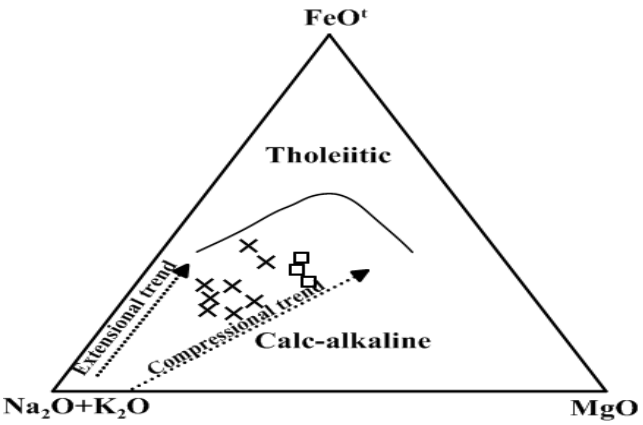

Fig (25) The AFM diagram for the studied granitoids, after [9]. The compressional and extensional trend [19].

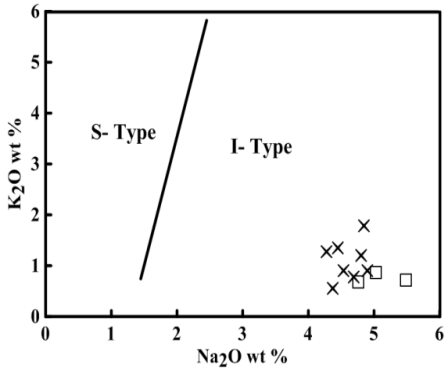

Fig (26) K_2O vs.Na_2O diagram for the studied granitoids. Boundary between i-type and s-type granites [17].

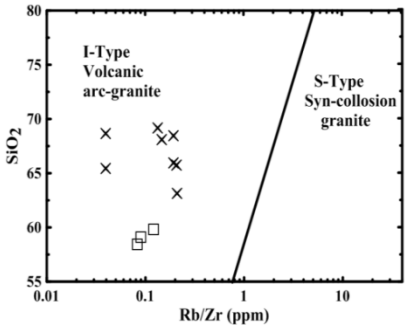

Fig(27) Rb/Zr-SiO_2 diagram for the studied granitoids [21].

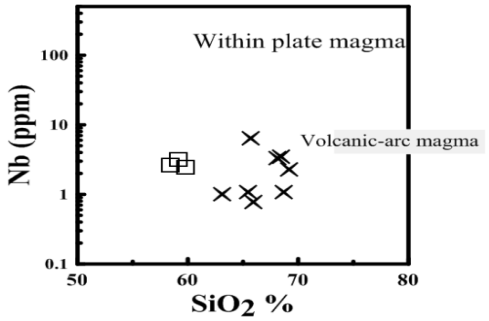

Fig(28) Nb versus SiO_2 diagram for the studied granitoids. Fields [11].

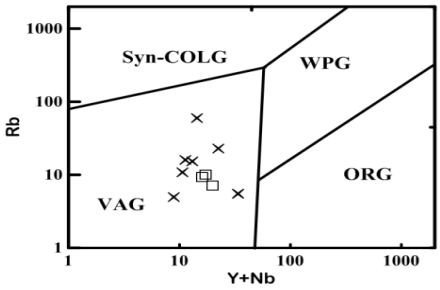

Fig(29) Rb versus (Y+Nb) discrimination diagram for the studied granitoid rocks, [24].

C. Rb- (Y+Nb) diagram

[24] proposed a bivariete tectonic discrimination diagram using the relation Rb (ppm) versus Y+Nb (ppm) **Fig (29)** to discriminate between volcanic arc granites (VAG), syn-collision granites (syn-COLG), oceanic ridge granites (ORG) and within plate granites (WPG) tectonic settings. The data points of the investigated granitoids fall mainly within the VAG field, due to their low abundances of Rb, Nb and Y.

5. Structural features and metamorphism of the area

Finally, the study area was affected by faults trending NE-SW and NNW-SSE. These faults underwent major rejuvenation after the emplacement of Phanerozoic of the rocks. Concerning, the metamorphism, only the Muiswirab metagabbros were partially acted upon by processes of the three phases of metamorphism such as uralitization, flasering, amphibolitzation and finally retrograde of amphibolite.

6. Conclusions

The present metagabbros include two varieties, which are similar in their composition to olivine gabbro norite and gabbro norite. They always have tholeiitic affinities and the scattering of their plots between MORB and island-arc tholeiite field is a good evidence for transitional tectonic environment. Moreover, the studied metagabbros in general exhibit low Ti , Zr and Nb contents. Generally, they have similarities with the ophiolitic gabbros elsewhere. [25] stated that “Zr, Ti, and Nb contents of the gabbroic rocks of ophiolite from Eastmost of the Arabian Shield is too low even for the back-arc marginal basin setting, commonly invoked for ophiolite genesis”. Accordingly, this may indicate that the present metagabbros were generated in the marginal basin.

Finally, [26] suggested that “ophiolites generated at major ocean ridges are unlikely to be immediately overlain by sediments with significant volcanic components, whereas such detritus may lie directly on arc-incipient, arc, and back-arc ophiolites”. Accordingly, the widespread distribution of the volcanogenic metasediments in the studied area and beyond its limits is a further

support of marginal regime during the Late Proterozoic time in this part of the Nubian Shield.

Generally speaking this conclusion is in agreement with the data obtained by [27] who stated that, the island arc marginal basin system could explain the past tectonic environment for the metagabbros of the Eastern desert of Egypt. On the other hand the present data is quite similar to the data obtained by [28] who considered that Jabal Al Wask (West of Saudi Arabia) as formed in a back-arc environment.

Concerning to the granitic rocks [29] classified the Egyptian granites into three groups G_1, G_2 and G_3 based on field relations, petrography, geochemical character and tectonic setting. G_1 group includes the older or syn-orogenic granites. G_2 group includes the younger or post-orogenic granites, while G_3 group includes some alkali granites and peralkaline granites.

Accordingly, and taking into consideration all the characteristics of the studied granitoids mentioned above the gneissic quartz diorite and gneissic tonalite can be classified as G_1 granite.

Geochemically, the investigated granitoids are of calc-alkaline nature, metaluminous and pertaining to I-type granites; furthermore, they have been generated under compressional environment above subduction zone and evolved in a volcanic-arc setting characterizing the orogenic belts.

Finally, the study area was affected by faults trending NE-SW and NNW-SSE. These faults underwent major rejuvenation after the emplacement of Phanerozoic of the rocks. Concerning, the metamorphism, only the Muiswirab metagabbros were partially acted upon by processes of the three phases of metamorphism such as uralitization, flasering, amphibolitzation and finally retrograde of amphibolite.

Reference

[1] EGSMA, Geologic map of Jabal Hamata Quadrangle, Egypt. Scale 1:250,000, Egyptian Geological Survey and Mining Authority, Cairo, Egypt, 1997.

[2] T. F. W. Barth, The feldspar geologic thermometers.: Norsk Geol. tidsskr, vol.42 (Feldspar volume), pp. 330-339, 1962.

[3] V. Dietrich, , R. Emmermann, R. Oberhänsli and H. Puchelt, Geochemistry of basaltic and gabbroic rocks from the West Mariana Basin and the Mariana Trench. Earth and Planetary Science Letters, Vol.39(1), pp.127-144, 1978.

[4] K. G. Cox, J. D. Bell and R. J. Pankhurst, 1979, The interpretation of igneous rocks. George. Allen and Unwin, London, pp. 468.

[5] M. Wilson, Igneous Petrogenesis. A global tectonic approach. Unwin Hyman, London. Pp.466, 1989.

[6] A. Miyashiro, Nature of alkalic volcanic rock series. Contributions to Mineralogy and Petrology, Vol.*66*(1), pp.91-104, 1978.

[7] A. Streckeisen, To each plutonic rock its proper name: Earth Science Reviews, vol.12, pp. 1-33, 1976.

[8] C. P. Thornton, and O. F. Tuttle, Chemistry of igneous rocks, I: Differentiation Index: Am. J. Sci., Vol. 258, pp.. 664-684, 1960.

[9] T. N. Irvine, and W. R. A. Baragar, A guide to chemical classification of the common volcanic rocks. Canada: J. Earth Sci., Vol. 8, pp. 523-548, 1971.

[10] A. Miyashiro, and F. Shido, Tholeiitic and calc-alkalic series in relation to the behaviors of titanium, vanadium, chromium and nickel: Am. Science, Vol. 275, pp. 265-27, 1975.

[11] J. A. Pearce, and G. H. Gale, Identification of ore-deposition environment from trace element geochemistry of associated igneous host rocks: Geological Society of London Special Publication, Vol. 7, pp. 14-24,1977.

[12] P. A. Floyd, and J. A. Winchester, Identification and discrimination of altered and metamorphosed volcanic rocks using immobile elements. Chem Geol 21: pp.291–306, 1978.

[13] W. Bloxen and A.D. Lewis, Ti, Zr, and Cr in some British pillow lavas and their petrogenetic affinities. Nature (Phys. Sci.) 237, pp.134–136, 1972.

[14] E. M. Taylor, Recent volcanism between Three-Fingered Jack and NorthSister, Oregon Cascade Range: Ore Bin, v. 27, p. 121-47.

[15] R. Berlin and C. M. B. Henderson, 1969, The distribution of Sr and Ba between the alkali feldspar, plagioclace and groundmass phases of porphyritic trachytes and phonolites. Geochim. Cosmochim. Act 33, pp.247-255, 1965.

[16] P. C. Bateman and F.C.W. Dodge, 1970,Variations of major chemical constituents across the central Sierra Nevada batholith. Geol. Soc. America Bull., 81:pp.409-20.

[17] D. R. Hunter, F. Barker, and H. T. Millard, The geochemical nature of the Archean ancient gneiss complex and granodiorite suite, Swaizland: A preliminary study: Precambrian Res., vol.7, pp. 105-127, 1978.

[18] F. Barker, Trondhjemites, dacites and related rocks. Amsterdam, Elsevier, pp.414, 1979.

[19] W. L. Petro, T. A. Vogel, and J. T. Wilband, Major elements chemistry of plutonic rocks from compressional and extensional plate boundaries.: J. Chem. Geol., vol.26, pp. 217-235,1979.

[20] R. Hine, I. S. Williams, B. W. Chappell, and A. J. R. White, Contrasts Between I- and S-

Type granitoids of the Kosciusco Batholith.: J. Geol. Soc. Aust., vol.25, pp. 219-234, 1978.

[21] N. B. W. Harris, C. J. Hawkesworth, and A. C. Ries, Crustal evolution on Northeast and East Africa from model Nd ages: Nature, vol. 309, pp. 773-776, 1984.

[22] I. G. Gass, Evolutionary model for the Pan-African crystalline basement: I. A.G. Bull., (Jeddah), vol.3, pp. 11-20,1979.

[23] A. E. Ringwood, The petrological evolution of island arc systems. Journal Geological Society London Vol.130, pp.183-204, 1974.

[24] J. A. Pearce, S. J. Lippard, and S. Roberts, Characteristics and tectonic significance of supra-subduction zone ophiolites: In: Kokelaar, P.B., Howells, M.F. (Eds.), Marginal Basin Geology. Geological Society, London, Special Publication, vol. 16, pp. 77–94, 1984.

[25] A.M. Al-Shanti and I.G. Gass, The Upper Proterozoic ophiolite mélange zones on the easternmost Arabian shield. Journal of the Geological Society of London Vol.140, pp.867–876, 1984.

[26] L. C. Evan, Island arc elements and arc-related ophiolites. Tectonophysics Vol.106 (3-4), pp.177-203, 1984.

[27] M.F. Ghoneim, M.A. Takla and E.M. Lebda, The gabbroic rocks of the central Eastern Desert, Egypt: a geochemical approach. Ann. Geol. Surv. Egypt XVIII, pp.1–22, 1992.

[28] A. R. Bakor, I. G. Gass, and C. R. Neary, Jabal al Wask, northwest Saudi Arabia: An Eocambrian back-arc ophiolite:Earth Planet. Sci. Letters, vol.30, pp. 1-9, 1976.

[29] A. A. Hussein, M. M. Ali, and M. F. El Ramly, A proposed new classification of the granites of Egypt.: J. Volcan. & Geoth. Research, vol.14, pp. 187-198, 1982.